The Role of the Protons and the Electrostatic Potential in the Reactivity of the (110) Sulfated Zirconia Surface

Joel Ireta,[†,‡] Felipe Aparicio,[†] Margarita Viniegra,[†] and Marcelo Galván*[,†,§]

Departamento de Química, División de Ciencias Básicas e Ingeniería, Universidad Autónoma Metropolitana-Iztapalapa, A.P.55-534, México, D.F. 09340, México, and Programa de Ingeniería Molecular, Instituto Mexicano del Petróleo, Eje Central Lázaro Cárdenas No. 152, A.P. 14-805, México, D.F. 07730, México

Received: August 27, 2002; In Final Form: November 19, 2002

Several models for the adsorption of H_2SO_4 on (110)-ZrO_2 surface were studied by total energy pseudopotential calculations, based on density functional theory. The analysis of the results focuses on the implications of the properties of the sulfated surface in its catalytic activity with hydrocarbons. The structural features of the models studied were in agreement with recently reported data on (101) and (001) faces of this material. The comparison of some properties of the sulfated surface with those of the hydroxylated one shows that one of the main features of sulfated zirconia (SZ) surface is its strong electrostatic potential around the sulfate group. This potential is intense enough to polarize hydrocarbons in the initial steps of their interaction with the surface. By combining this effect with the impact of proton detachment, a model for the interaction of SZ surface with hydrocarbons emerged. This model stresses the importance of adsorbed protons in the activity, and allows us to rationalize the dependence of the latter on the water content in the reaction environment.

Introduction

Since it was discovered that sulfated zircona (SZ) has a high capacity for catalyzing reactions as paraffin isomerization, under much milder conditions than those used with conventional catalysts,[1,2] the SZ has been the subject of numerous studies dedicated to characterize their physicochemical properties in order to understand the nature of its strong acidity.[3] Despite the tremendous amount of work done, the strength, the nature, and the structure of SZ acid sites are still a matter of controversy.[3] Some characterization of its Brønsted sites led to the conclusion that SZ has superacidic protons, making this catalyst more acidic than 100% sulfuric acid.[4−6] In contrast to those conclusions, several authors claimed that SZ is not a superacid,[7−9] and that its acidity is weaker than HZSM-5 zeolite.[8,9] Other reports indicate that the activity of SZ in butane isomerization is not related to Brønsted acidity, but is related to the oxidation capacity of SZ,[10−12] which involves Lewis acidity. However, the presence of protons in the reaction environment is required for the system activity.[13,14] Some authors mention that the strong acidity of sulfated zirconia is due to a combination of Lewis and Brønsted acid sites.[15,16] Along that vein, it was proposed that the maximum catalytic activity of SZ is reached when there is a 1:1 ratio of Brønsted and Lewis sites on the catalyst.[15]

In relation to the structural characteristics involved in the catalytic activity of sulfated zirconia, it is well-known that sulfated tetragonal phase is active in butane isomerization,[17] and only recently it has been shown that the sulfated monoclinic phase is active too.[18,19] Results based on high-resolution transmission electron microscopy show that sulfation not only stabilizes the tetragonal phase of zirconia at room temperature, but also induces the formation of well-faceted small zirconia crystallites, with the predominance of (110) terraces.[20] Likewise, in SZ stabilized by Fe/Mn the (101) and (001) facets are also observed.[21,22]

Several spectroscopic and surface characterization techniques have been applied to SZ for determining the active species on the surface. According to those results, it has been suggested that sulfate or bisulfate in 2-fold[23] or 3-fold[6,24] coordination, as well as SO_3,[25] could be present on the zirconia surface. Recently, the (101) and (001) faces of tetragonal SZ were studied using ab initio molecular dynamics;[9] it was shown that sulfate anion and SO_3 in a 3-fold adsorption are the most stable species depending on whether sulfuric acid was adsorbed on the (101) or the (001) face, respectively.

In this work a theoretical study of various models for the adsorption of sulfuric acid on the (110) surface of tetragonal zirconia, using ab initio total energy calculations,[26] was carried out. Although the (110) face is not the most stable bare surface in tetragonal zirconia,[27] there is experimental evidence showing that this face is present in SZ samples.[20] In this context this study is somehow complementary to those of Haase and Sauer[9] and of Kanougi et al.[28]

Since infrared spectroscopy is one of the most frequently applied techniques to study SZ, a comparative analysis of the proton and S═O vibrational frequencies among the different models of sulfated and full hydroxylated zirconia (OHZ) was performed. Also, calculations of the electronic structure of methane in the presence of sulfated and hydroxylated zirconia were performed. On bases of these results, the possible relation between the high positive electrostatic potential on the sulfur atom, and the capacity of the sulfated zirconia for catalyzing the paraffin isomerization reaction is discussed.

* Corresponding author. Fax: (525) 804-4666. E-mail: mgalvan@xanum.uam.mx.

† Departamento de Química.

‡ Present address. Fritz-Haber-Institut der Max-Planck-Gesellschaft, Faradayweg 4-6, D-14195 Berlin-Dahlem, Germany.

§ Programa de Ingeniería Molecular.

10.1021/jp026852y CCC: $25.00
Published on Web 12/21/2002

TABLE 1: Lattice Parameters for Cubic and Tetragonal Bulk Phases of Zirconia, and Bond Lengths for ZrO Molecule in Ångstroms

		tetragonal		
	cubic fcc *a*	*a*	*b*	molecule
calcd	5.01	3.58	5.24	1.70
exptl	5.09[a]	3.64[b]	5.2[b]	1.71[c]

[a] Reference 34. [b] Reference 35. [c] Reference 36.

Computational Aspects

Ab initio calculations were performed with Density Functional Theory (DFT) in the context of the local approximation to the exchange-correlation functional and pseudopotentials (TEPC).[26,29] This methodology has been proved to be useful for studying bulk phases and different surfaces of zirconia.[27,30,31] As the main objectives of this work are not related to detailed energetic aspects, but to properties that are correctly described by the local density approximation (LDA), all the calculations were done within this level of theory. The pseudopotentials used in this work were generated following RRKJ scheme[32] and tested in small molecules (see Ireta and Galván[33] and Table 1), and in the zirconia bulk phases (Table 1). The oxygen and sulfur pseudopotentials were generated at 40 Ry cutoff with six valence electrons each. For zirconium, a 50 Ry cutoff and four valence electrons were used. It is known that, for a very accurate description of zirconium, the inclusion of (4s,4p) core states is required.[31,37] However as it was shown by Christensen and Carter,[27] and the results in Table 1, reliable calculations can be performed including only four valence electrons. The generated pseudopotentials were cast into the Kleinman and Bylander form with s channel as the local potential.[38] For the calculations of the sulfuric acid adsorption models, two special k-points were used for sampling the first Brillouin zone.[39] Increasing the sampling from two to four special k-points, led to a change in energy of around 0.003 eV. Thus, it can be considered that two k-points are enough to describe the system correctly. In the case of the calculations for methane in the presence of OHZ and SZ, only one k-point was used because the unit cell for these systems are four times bigger than the unit cell for SZ. Within the TEPC methodology, the Kohn−Sham orbitals at each k-point are expanded in terms of a discrete plane-wave basis set.[26] In this work, the plane wave expansion was set using an energy cutoff of 50 Ry. The Kohn−Sham equations in reciprocal space were solved according to the method developed by Arias et al. [40]

Adsorption Models

The (110) tetragonal zirconia surface was modeled with the supercell technique,[41] (Figure 1). In the model, a vacuum thickness of at least the double of the slab width was used. The slab was constructed by cleaving the crystallographic bulk cell of tetragonal zirconia along the (110) plane. In a recent study of tetragonal zirconia surfaces, it was mentioned that a slab containing five oxygen and four zirconium atomic layers is necessary to obtain convergence in the surface energy of the system.[27] However, in this work four oxygen and three zirconium atomic layers in the slab model were considered (see Figure 1). This slab thickness generates reliable geometry for the adsorbed species, which was tested calculating one of the adsorption models using a bigger slab (the geometry agreed within a range of 0.01 Å). Moreover, the density of states (DOS) is well-described even with the smallest slab (Figure 2). The surface was partially oxygen terminated in order to be stoichiometric and nonpolar.

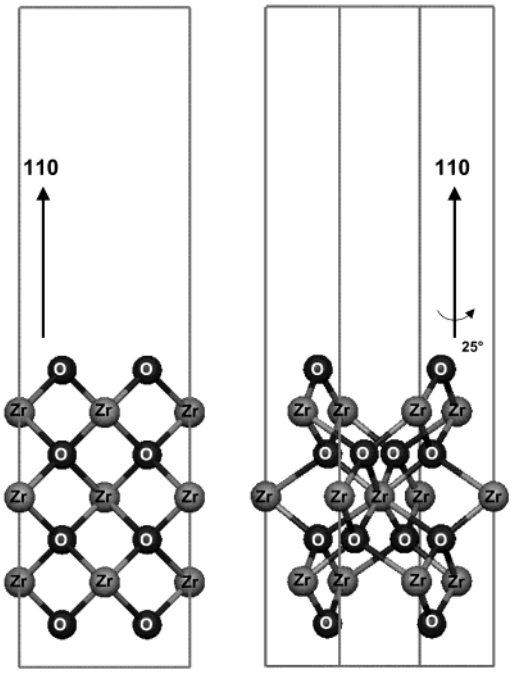

Figure 1. Supercell used for modeling the (110) tetragonal zirconia surface. The size of the unit cell is 5.15 Å × 5.27 Å × 20 Å; in the longest direction 12.5 Å corresponds to the vacuum. The periodic image of the boundary atoms are explicitly shown. This supercell contains six zirconium and 12 oxygen atoms, distributed as follows: two zirconium atoms in each zirconium-atomic layer, two oxygen atoms in the first and the last oxygen-atomic layers, and four oxygen atoms in each intermediate oxygen-atomic layer. The right part is a view of the supercell of the left panel, rotated 25° around the (110) axis.

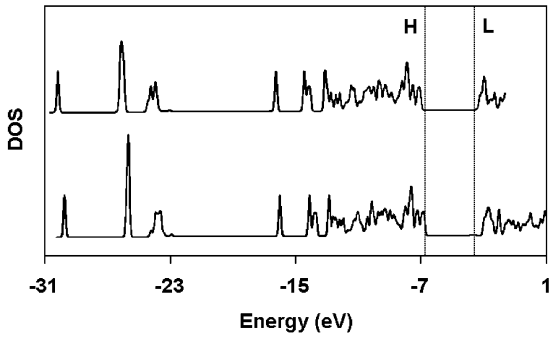

Figure 2. Regional densities of states obtained from a slab containing five O layers and four Zr layers (upper DOS), and the slab used throughout this paper (lower DOS). A region including the adsorbate and the first three surface atomic layers was considered for calculating the DOS. H and L labels indicate the HOMO and the LUMO band-edges positions, respectively.

In this work the adsorption of sulfuric acid on the (110) tetragonal zirconia face was studied using one side, 2-fold and 3-fold sulfate adsorption models, as well as the bisulfate in a 2-fold coordination. The 2-fold adsorption models were built up locating the oxygen atoms of sulfate or bisulfate, in lattice sites where an oxygen was removed in the construction of the partially oxygen terminated surface model. In the 3-fold case, two oxygen atoms of sulfate were located as above, and the third one replacing a surface oxygen. The replaced surface oxygen was shifted up, to a corresponding lattice position as if it were in the next bulk like oxygen layer. In all the models sulfuric acid protons were located on the topmost surface-oxygen atoms, resembling a partial or a complete sulfuric acid deprotonation. Likewise, a model for a fully hydroxylated (110) tetragonal zirconia face was built up by locating hydrogen atoms

TABLE 2: Distances on the Sulfate Adsorption Models in Ångstroms[a]

	A model	B model	C model
$S-O_1$	1.47	1.44	1.47
$S-O_2$	1.47	1.53	1.56
$S-O_3$	1.55	1.54	1.51
$S-O_4$	1.56	1.53	1.52
O_2-Zr_3		2.28	
O_2-Zr_4		2.51	
O_3-Zr_1	2.22	2.16	2.33
O_3-Zr_3	2.61	2.19	2.55
O_4-Zr_2	2.56	2.28	2.60
O_4-Zr_4	2.21	2.18	2.24
O_5-Zr_3	2.07	4.63	1.98
O_5-Zr_4	2.24	2.20	2.07
O_6-Zr_1	2.25	2.14	2.38
O_6-Zr_2	2.08	2.07	2.13
H_1-O_2			0.99
H_1-O_5	1.04	0.98	
H_2-O_6	1.02	1.05	0.99

[a] See Figure 3 for atom label identification.

TABLE 3: Nonbonded O−H Distances on Sulfate Adsorption Models, in Ångstroms[a]

	A model	B model	C model
H_1-O_2	1.48		
H_2-O_1	1.59		1.92
H_2-O_5		1.49	

[a] See Figure 3 for atom label identification

on the topmost surface oxygen atoms, and hydroxyl species in lattice sites where oxygen atoms were removed. This model corresponds to the dissociation of two water molecules on the zirconia surface. In all the cases the relaxed structures were obtained by moving the coordinates of the first three atomic layers, and those of the adsorbed species.

For methane calculations in the presence of hydroxylated and sulfated zirconia, a unit cell corresponding to a 2×2 surface unit cell was used in order to have enough room for the adsorbates. Methane was located above the surface regions with the strongest positive electrostatic potential. As the purpose of these calculations was to study the perturbation effect of O−H and SZ on the electronic structure of methane, no relaxation of the geometries was carried out.

Results

1. Sulfated Zirconia. In Figure 3a−c, the relaxed adsorption models for sulfuric acid are shown. The 2-fold sulfate coordination (A model) is more stable than the 3-fold sulfate (B model) and the 2-fold bisulfate (C model) adsorption models by 9 and 22.9 kcal/mol, respectively. In all of the cases, there is at least one oxygen−sulfur distance (Table 2) that compares with the S═O bond length in the sulfuric acid molecule (1.44 Å) or with the bisulfate anion (1.47 Å). Two different hydroxyl-bond lengths in the models are noticed (see Table 2). The shortest, that is present in the bisulfate model and the 3-fold sulfate adsorption, resembles the bond length found for the hydroxyls in the sulfuric acid molecule and bisulfate anion (0.96 Å). The longest one is related to those hydrogen atoms that seem to be involved in hydrogen bonds (H1 and H2 in A model, and H2 in B model). They are close enough to other oxygen atoms (O1 and O2 in A model, and O5 in B model when periodic boundary conditions are applied), to form such kind of bonds (see Figure 3 and distances in Table 3). It was considered that a sulfate oxygen is bound to a surface zirconium atom when the distance between them is shorter to or equal to the longest Zr−O bond in zirconia bulk (2.46 Å). Thus the O3 and O4 atoms of the 2-fold models are bound only to one zirconium atom each (Figure 3a,c) whereas in the 3-fold case they are bound to two zirconium atoms each (Figure 3b). Therefore, it may be concluded that the 8-fold bulk like coordination of surface Zr atoms is restored only by the 3-fold adsorption of sulfate. This model forms the shortest bonds with the surface (see Zr−O distances in Table 2), however it is not the most stable one. The 2-fold adsorption (A model) is 9 kcal/mol more stable than the 3-fold adsorption (B model). This small energy difference is not big enough to distinguish which of the models will be the most stable at reaction conditions, then both 2-fold and 3-fold sulfates might be present on the surface. As it will be treated in detail in the vibrational analysis section, the coexistence of these two adsorption structures can be related to the presence of two vibration frequencies in the S═O stretching region.[19] The extra energy stabilization in the A model may arise from the presence of the hydrogen bonds discussed above. The surface−complex geometries obtained in this work are in close agreement with those reported by Haase and Sauer,[9] despite the different faces used in that study, as well as the different slab thickness criteria for modeling the surface.

In relation to the electronic structure of the various sulfated zirconia models, the main contribution to the highest occupied orbitals (HOMOs) comes from the O5 and O6 oxygen atoms (see Figure 3a,b). To a lesser extent the double-bounded oxygen atoms in the sulfate group (O1, O2 in Figure 3a and O1 in Figure 3b) participate in the HOMOs as well. The contribution to the lowest unoccupied orbitals (LUMOs) mainly comes from the topmost surface-zirconium atoms.

As was pointed out in the Introduction, the presence of adsorbed protons on the surface is important for its reactivity. One way to simulate the lack of protons, without requiring the use of a nonneutral unit cell, is to remove the H atoms attached to the hydroxyls group of the surface to a non bonded distanced. In fact, some changes in the peaks of the density of states related to the frontier orbitals (HOMOs and LUMOs) were observed when the protons of the hydroxyl groups were moved 2 Å away from the surface. The eigenvalues of the HOMO and LUMO orbitals were shifted toward higher energies in variable extent depending on the proton that was moved (Figure 4). Thus, the protons of the hydroxyl groups help the LUMOs to be energetically more accessible, and this might have implications in the reactivity of the SZ, as will be discussed later.

2. Hydroxylated Zirconia. Regarding the relaxed structure of hydroxylated zirconia (Table 4 and Figure 3d), the hydroxyls on the surface are distinguished by their O−Zr distance. The O_1-H_3 and the O_2-H_4 are farther from the surface than the other two hydroxyls (O_4-H_2 and O_3-H_1), but close enough to restore the 8-fold bulklike coordination of the surface zirconium atoms (considering the same binding criteria as in SZ coordination analysis). However, the O−H bond lengths are not affected by the O−Zr distance, being the same for all of the hydroxyls (0.98 Å).

3. Vibrational Analysis. The calculated stretching vibrational frequencies for S═O and O−H of the sulfate adsorption models and of the hydroxylated zirconia are presented in Table 5. It is known that SZ exhibits a vibrational frequency at about 1400−1380 cm^{-1}, associated to an asymmetric stretch of S═O bond.[17] The values obtained in this work for these frequencies (Table 5) are a little higher than the experimental ones, but the error is in accordance to the average observed (7.4%), in calculations of vibrational frequencies with the TEPC methodology.[33] It is worth mentioning that we found different S═O vibrational

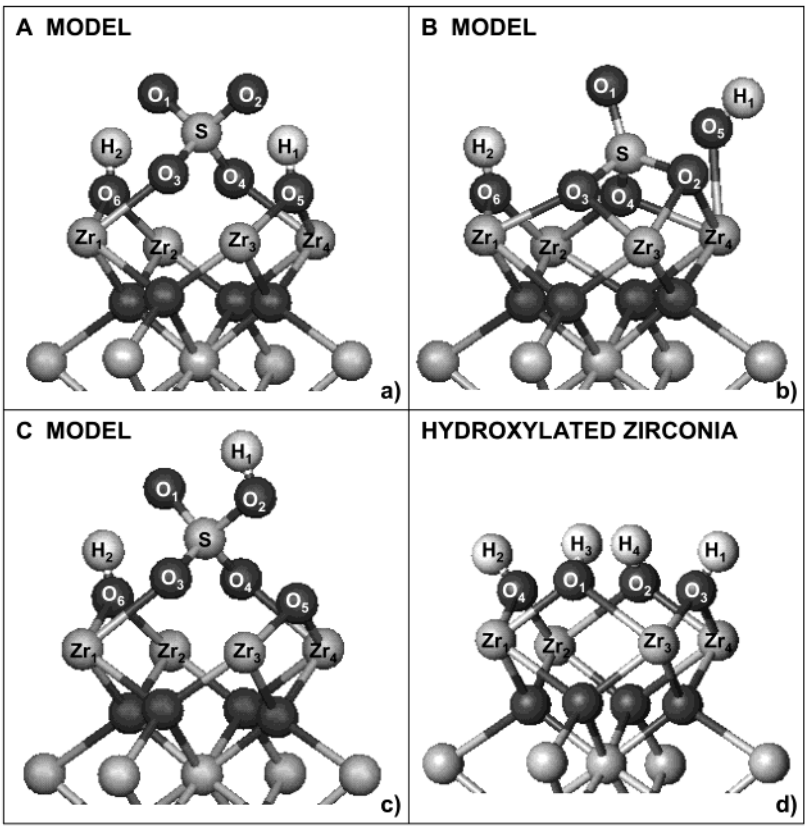

Figure 3. Sulfated and hydroxylated zirconia models. See text for label identification. At each panel only the atoms that were relaxed are shown. The structures orientations are according to Figure 1. The periodic image of the boundary atoms are explicitly shown, it means that Zr_1 is equivalent to Zr_4 and Zr_2 to Zr_3. Also, in (b) H2 is close enough to the periodic image of O5 to interact through a hydrogen bond.

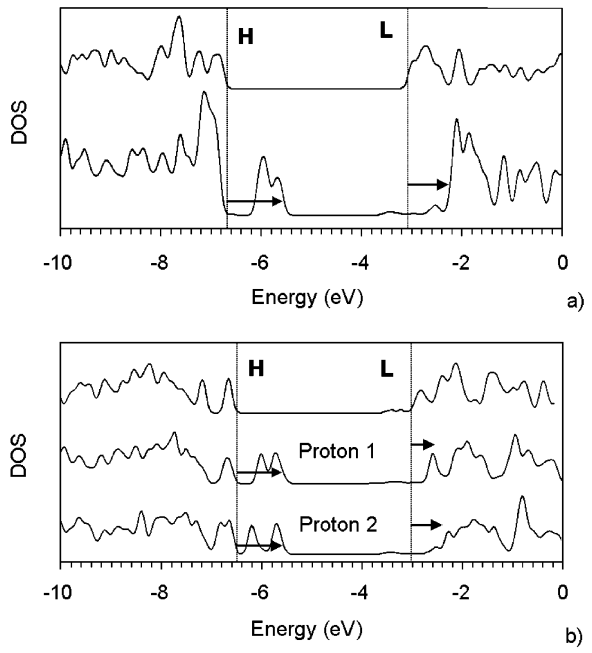

Figure 4. HOMO (H) and LUMO (L) shifts induced by proton detachment: a) for the A model, and b) for the B model. In the latter case the effect in the LUMO band is splitted according to the proton that was detached (see Figure 3b for proton identification). The proton detachment was done locating the hydrogen atom two angstroms far from its original equilibrium position along the (110) direction.

frequencies for models A and B. These two values could correspond to the experimental frequencies obtained in the sulfate region in sulfated zirconia.[19] With this assignation, one can say that the sulfate with triple coordination with the surface

TABLE 4: Distances on Hydroxylated Zirconia Model, in Å[a]

	OHZ
H_1-O_3	0.98
H_2-O_4	0.98
H_3-O_1	0.98
H_4-O_2	0.98
O_1-Zr_1	2.12
O_1-Zr_3	2.41
O_2-Zr_2	2.39
O_2-Zr_4	2.11
O_3-Zr_3	2.09
O_3-Zr_4	2.22
O_4-Zr_1	2.23
O_4-Zr_2	2.09

[a] See Figure 3d for atom label identification.

TABLE 5: Calculated Vibrational Frequencies in cm^{-1} [a]

bond	A model	B model	C model	OHZ
S=O	1399 (asymmetric)	1492		
O−H	(O_5-H_1) 2536	(O_5-H_1) 3527	(O_1-H_2) 3387	(O_3-H_1) 3552
	(O_6-H_2) 2861	(O_6-H_2) 2461	(O_6-H_2) 3390	(O_1-H_3) 3567

[a] See Figure 3 for atom label identification.

corresponds to the higher value in cm^{-1}. The reported O−H frequencies on hydroxylated and sulfated zirconia are 3670 and 3640 cm^{-1}, respectively.[42] Accordingly, some of the calculated O−H frequencies agree with the experimental values within the error of the method (O−H of OHZ and O_5-H_1 of B model, see Table 5). The O−H frequencies of A model and that of O_6-H_2 for the B model, are about 1000 cm^{-1} lower than the experimental value. This shift toward lower frequencies can be

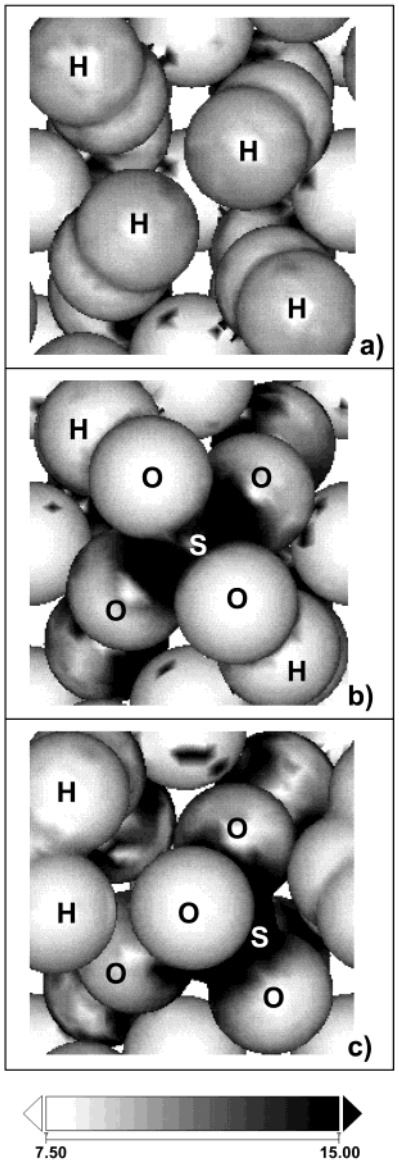

Figure 5. Top view of electrostatic potential projections onto an overlapping surface setup as a superposition of spheres of 1 Å radii, and centered in the nuclei positions: (a) for hydroxylated zirconia, (b) for A model of sufated zirconia, (c) for B model of sulfated zirconia. The (110) face is shown in each panel. The scale corresponds to eV.

related to the formation of hydrogen bonds described in section 1. For the bisulfate adsorption (C model), the frequencies of the hydroxyl groups are shifted toward lower values about 200 cm^{-1} respect to the frequencies of hydroxyls in OHZ and O5−H1 of B model. This is connected to the elongation of O−H bonds observed for hydroxyls in C model, which are 0.01 Å larger than those of OHZ or O5−H1 (compare values in Table 2 and Table 4).

4. Methane Interaction with Sulfated and Hydroxylated Surfaces. One interesting feature of SZ is the strong positive electrostatic potential on the sulfate group induced by the surface (see Figures 5 and 6). It seems that sulfate group suffers such a polarization that the shielding effect of the electronic cloud around its nucleus is diminished. This effect is more noticeable in the sulfur atom (see Figure 5). The positive electrostatic field on sulfur is at least twice the value of the electrostatic field in OHZ, and about 2 orders of magnitude higher than that on the sulfur of sulfuric acid, comparing them at 1.0 Å away from atom nuclei in both cases. Indeed, the electrostatic field of the

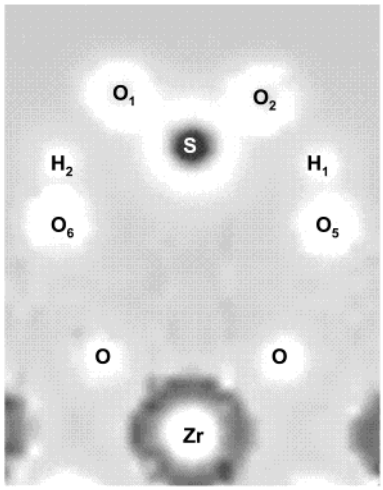

Figure 6. Lateral view of the electrostatic potential for the model A of sulfated zirconia on a plane containing the sulfur and zirconium atoms. The vertical axis in the figure is aligned to the (110) direction. The gray areas correspond to values of the electrostatic potential ranging from 0 to 30 eV values and the white regions contain values from 0 to −10 eV.

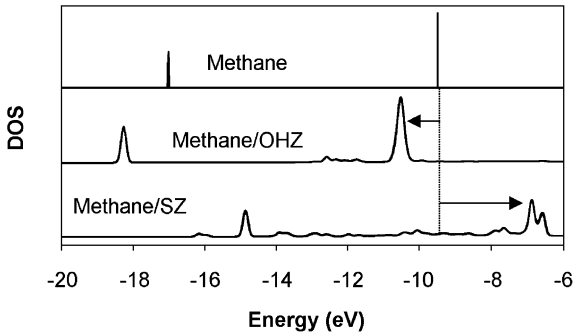

Figure 7. Methane HOMO shift induced by the hydroxylated (OHZ) and sulfated (SZ) zirconia surfaces. The shifts are indicated by the arrows and the DOE's were aligned by their Fermi levels.

3-fold sulfate adsorption model is slightly higher than that observed on the 2-fold model. In contrast to the electrostatic potential around Zr atom, which is more diffuse, around the sulfur atom it is more concentrated close to the nucleus. As a first step to investigate if the strong catalytic activity of the SZ in butane isomerization could be related to the strong electrostatic potential on the sulfate of SZ, the perturbative effect of the SZ (A model) on the methane electronic structure was calculated. Similar calculations were carried out replacing SZ by OHZ in order to have a reference system, which is not active. In the calculation of methane over the A model of SZ, the closest methane-hydrogen atom to the surface was located 1.5 Å above sulfate group and pointing toward the sulfur atom. Thus, the distance among that methane-hydrogen and the closest sulfate-oxygen atoms are about 1.65 Å, and between methane-hydrogen and sulfur is 1.95 Å. In that position the methane-hydrogen, in principle, could not be involved in covalent bonds with sulfate-oxygen atoms (see i.e., the O−H bond distance for bisulfate in C model, Table 2), but may develop hydrogen-bonds. In the case of OHZ two calculations were carried out; in both, the closest methane-hydrogen atom to the surface was located 1.5 Å above O−H groups, and pointing toward the middle point between similar surface hydroxyls (between O_1-H_3 and O_2-H_4, or O_3-H_1 and O_4-H_2).

In Figure 7 the DOS of "free" methane molecule as well as the DOS of methane in the presence of OHZ and SZ are shown.

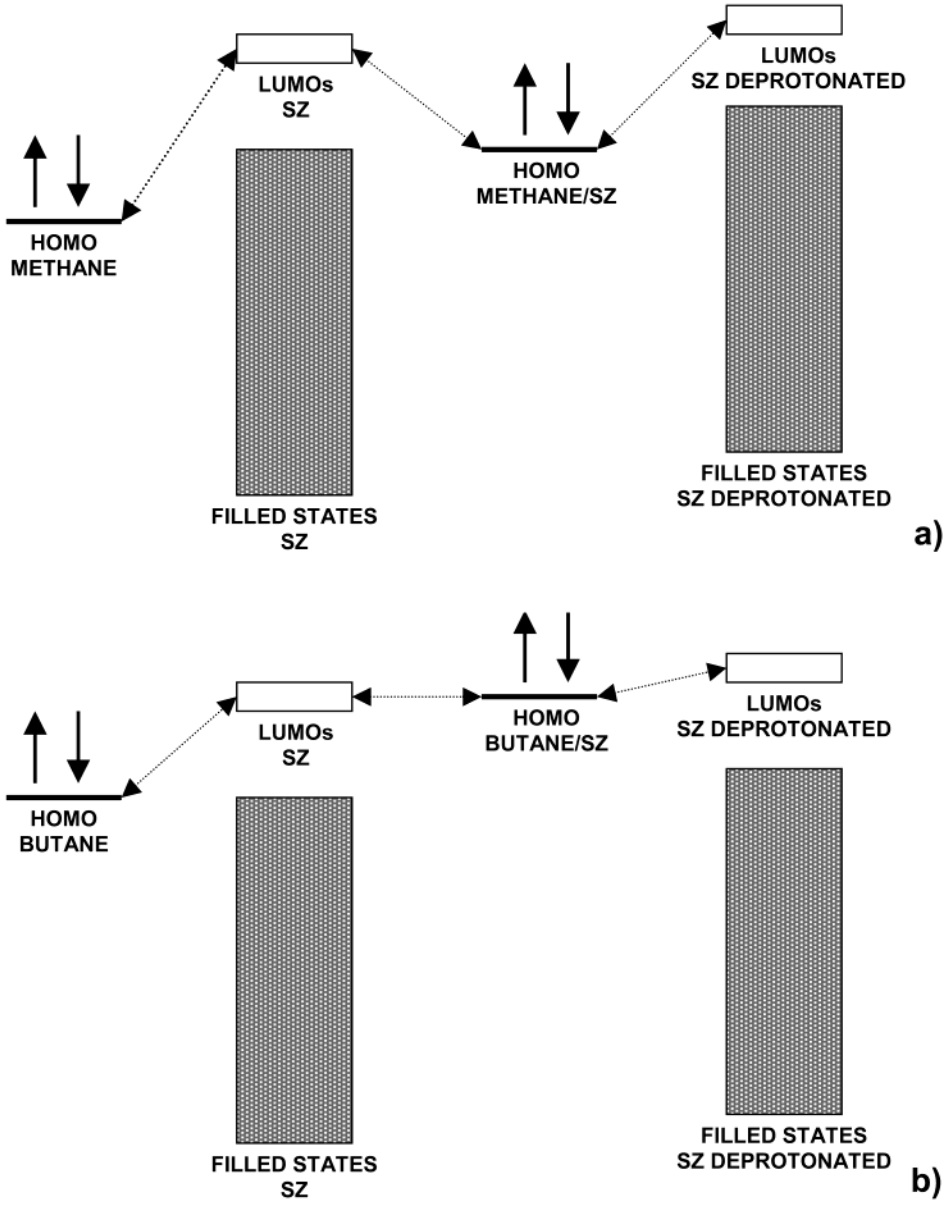

Figure 8. Schematic representation of the relative positions, in an energy scale of the eigenvalues of the HOMO orbitals of the (a) methane or (b) butane, and the LUMOs of the sulfated zirconia. The positions correspond to the calculations done, except for the butane HOMO shift which was supposed to be the same as that of methane HOMO.

In this figure it is noticed that the hydroxylated surface pushes down the HOMO eigenvalues of methane by 0.6 eV, but the sulfated surface produces the contrary effect, pushing up these eigenvalues about 3 eV. The effects on the electronic structure of methane induced by SZ could be related to possible hydrogen bonds among methane−hydrogen and sulfate−oxygen atoms or to the strong electrostatic potential on sulfur and oxygen atoms.

Discussion

Butane isomerization on SZ has been proposed as a surface chain reaction that, at low temperatures, has a bimolecular mechanism involving C_8 species.[43,44] Several processes may generate the reactive intermediates: protolysis of butane, dehydrogenation of butane, or by the oxidation of this hydrocarbon.[44] Brønsted and/or Lewis catalysis could be implicated in such processes, but according to recent experimental[8] and theoretical calculations,[9] the surface protons on SZ are not superacid; therefore, a simple Brønsted catalysis would not be directly responsible for the SZ activity. This points toward Lewis catalysis, though there is no convincing evidence for a charge transfer process, which is mainly related to Lewis catalytic activity.

To explore the viability of such processes, the adsorbate−surface electronic interaction can be analyzed by the frontier orbitals theory.[45] As it is well-known this theory proposes that attractive interactions depend on the relative energy of the HOMOs and LUMOs as well as the symmetry and overlap quality of these orbitals.[46] From this point of view, two important results were obtained in this work: the sulfated zirconia shifts toward higher energy the HOMO of methane, and the protons of hydroxyls shift toward lower energies the LUMOs of the SZ; in both cases the relative energy between their frontier orbitals decreases (Figure 8a). Therefore both effects tend to favor a methane−SZ interaction. However, it is known from the experiment that methane does not interact with SZ, but butane does. At this point it is interesting to describe eigenvalue differences between the LUMOs of the surface and the HOMO

of methane and butane. The difference between methane-HOMOs and SZ-LUMOs is about 3 eV. Comparing the HOMO eigenvalue of the isolated methane with that of isolated butane, it is found that the latter is higher in energy by 3 eV. Therefore, if SZ surface induces an energy shift on butane HOMO at least similar to that observed for methane (it means an energy difference, between butane and surface frontier orbitals less than 1 eV), the butane−surface interaction would occur (Figure 8b). This attractive interaction could induce either an oxidation of butane, by a charge transfer or a hydride transfer (carbocation generation),[47] or a covalent butane−surface interaction. This kind of processes have already been proposed by other authors on the bases of experimental grounds,[10−12,47,48] and have been observed in other systems such as the sulfide-coordinated transition metal complexes.[49]

The abatement of the catalytic activity when water content is increased in the reaction environment[13,14] is another effect that could be induced by the strong electrostatic potential on SZ. It is known that the absence of water, as well as the excess of it, reduces the surface reactivity. According to theoretical results,[9,50] water molecules dissociate on zirconia, generating hydroxylated surfaces. By supposing that sites on SZ that were not covered by sulfate also deprotonates water (acting like bare zirconia), one can infer that, after a certain water content, hydroxyl saturation of the surface will be achieved. This process provides the required protons for surface activation. After saturation, additional water molecules in the medium could be physisorbed by the surface, screening the SZ strong electrostatic potential and diminishing, therefore, its catalytic activity. This possibility is supported by recent findings on a titanium dioxide surface.[51] Moreover, the effect produced by the lack of water on the reaction environment, i.e., the decrease in the catalytic activity, could be related to the deficiency of protons on the surface (which would shift the LUMOs of SZ as was pointed out in section 1 of the results), reducing the possibility of a charge transfer or the generation of a covalent bond between butane and SZ as was discussed above (see Figure 8b).

It is important to point out that as neither symmetry nor overlap of the frontier orbitals were considered, the latter discussion cannot be conclusive. On the other hand, it is known that the local approximation to the exchange and correlation functional underestimates the gaps,[52−54] mainly because the calculated HOMO eigenvalues are not as deeper as the expected values for the real systems; however, the trends of the eigenvalue shifts in which the above discussion is based on, will be preserved in a qualitative basis.

Conclusions

According to the results presented in this work, the 2-fold sulfate is the most stable adsorbed species on the (110) zirconia surface. The 3-fold adsorption could also be present in the temperature activated SZ, since the energy difference between 2-fold and 3-fold is only 9 kcal/mol and could be attributed to hydrogen bond formation. The strong electrostatic potential around the sulfate group induces a significant polarization on a methane molecule close to the SZ surface. It is important to stress that such polarization is not promoted by hydroxylated zirconia. This effect, together with the LUMO shift induced by the protons of the SZ-hydroxyl groups, favor a methane−surface interaction. This evidence suggests that SZ activity could involve in the first step a Lewis catalysis mainly related to the sulfate group, not to the support. It means that any support for sulfate that could induce such a high polarization of the electronic cloud of sulfur atom that unshield it could generate a catalyst that activates the C−H bond of hydrocarbons.

Finally, although in the 2-fold sulfate adsorption model there are not O−H frequencies close to the experimental values, because the unit cell is not big enough to adsorb a hydroxyl group far from the sulfate to avoid the hydrogen-bond formation, the vibrational analysis done in this work confirms that the proposed structures are reliable for modeling sulfate adsorption on zirconia, as was also obtained in ref 9. However, bigger unit cells should be used for exploring other adsorption models as well as for simulating butane−SZ interaction.

Acknowledgment. This work was supported in part by the Instituto Mexicano del Petróleo through FIES-95F-139-111 project, and by CONACYT through 400200-5-36482-E and 29095-E projects. J.I. and F.A. acknowledge CONACYT for Ph. D. scholarships. We thank Andrés Cedillo, Alberto Vela, and José Manuel Domingez for valuable discussions. We acknowledge DGSCA, UNAM, and Instituto Mexicano del Petróleo for giving us access to their computer facilities.

References and Notes

(1) Hino, M.; Kobayashi, S.; Arata, K. *J. Am. Chem. Soc.* **1979**, *101*, 6439.
(2) Hino, M.; Arata, K. *J. Chem. Soc., Chem. Commun.* **1980**, 851.
(3) Song., X.; Sayari, *A. Catal. Rev.−Sci. Eng.* **1996**, *38*, 329 and references therein.
(4) Yamaguchi, T.; Jin, T.; Tanabe, K. *J. Phys. Chem.* **1986**, *90*, 3148.
(5) Guisnet, M. *Acc. Chem. Res.* **1990**, *23*, 392.
(6) Riemer, T.; Spielbauer, D.; Hunger, M.; Mekhemer, G. A. H.; Közinger, H. *J. Chem. Soc., Chem. Commun.* **1994**, 1181.
(7) Adeeva, V.; de Haan, J. W.; Jänchen, J.; Lei, G. D.; Schümemann, V.; van de Ven, L. J. M.; Sachtler, W. M. H.; van Santen, R. A. *J. Catal.* **1995**, *151*, 364.
(8) Drago, R. S.; Kob N. *J. Phys. Chem. B* **1997**, *101*, 3360.
(9) Haase, F.; Sauer J. *J. Am. Chem. Soc.* **1998**, *120*, 13503.
(10) Yaluris, G.; Larson, R. B.; Kobe, J. M.; Gonzalez, M. R.; Fogash, K. B.; Dumesic, J. A. *J. Catal.* **1996**, *158*, 336.
(11) Ghenciu, A.; Farcasiu, D. *J. Chem. Soc., Chem. Commun.* **1996**, 169.
(12) Farcasiu, D.; Ghenciu, A.; Li, J. Q. *J. Catal.* **1996**, *158*, 311.
(13) Arata, K. *Adv. Catal.* **1990**, *37*, 165.
(14) Song, S. X.; Kydd, R. A. *J. Chem. Soc., Faraday Trans.* **1998**, *94*, 1333.
(15) Nascimento, P.; Akratopoulou, C.; Oszagyan, M.; Coudurier, G.; Travers, C.; Joly, J. F.; Védrine, J. C. *Stud. Surf. Sci. Catal.* **1993**, *75*, 1185.
(16) Morterra, C.; Cerrato, G.; Bolis, V.; Di Ciero, S.; Signoretto, M. *J. Chem. Soc., Faraday Trans.* **1997**, *93*, 1179.
(17) Morterra, C.; Cerrato G.; Pinna, F.; Signoretto, M. *J. Catal.* **1995**, *157*, 109.
(18) Vera, C.; Parera, J. M. *J. Catal.* **1997**, *165*, 254. Stichert W.; Schüth, F. *J. Catal.* **1998**, *174*, 242.
(19) Stichert, W.; Schüth, F.; Kuba, S.; Knözinger, H. *J. Catal.* **2001**, *198*, 277.
(20) Benaïssa, M.; Santiesteban, J. G.; Díaz, G.; Chang, C. D.; José-Yacamán, M. *J. Catal.* **1996**, *161*, 694.
(21) Benaïssa, M.; Santiesteban, J. G.; Díaz, G.; José-Yacamán, M. *Surf. Sci.* **1996**, *364*, L591.
(22) Morterra, C.; Cerrato, G.; Ferroni, L.; Montanero, L. *Mater. Chem. Phys.* **1994**, *37*, 243.
(23) Yamaguchi, T.; Jin, T.; Tanabe, K. *J. Phys. Chem.* **1986**, *90*, 3148.
(24) Bensitel, M.; Saur, O.; Lavalley, J.-C.; Morrow, B. A. *Mater. Chem. Phys.* **1998**, *19*, 147.
(25) White, R. L.; Sikabwe, E. C.; Coelho, M. A.; Resasco, D. E. *J. Catal.* **1995**, *157*, 755.
(26) Payne, M. C.; Teter, M. P.; Allan, D. C.; Arias. T. A.; Joannopoulos, J. D. *Rev. Mod. Phys.* **1992**, *64*, 1045.
(27) Christensen, A.; Carter, E. A. *Phys. Rev. B* **1998**, *58*, 8050.
(28) Kanougi, T.; Atoguchi, T.; Yao, S. *J. Mol. Catal. A: Chem.* **2002**, *177*, 289.
(29) In the present work the exchange and correlation potential used was set according to Perdew, P.; Zunger, A. *Phys. Rev. B* **1981**, *23*, 5048.
(30) Parlinsky, K.; Li, Z. Q.; Kawazoe, Y. *Phys. Rev. Lett.* **1997**, *78*, 4063.
(31) Králik, B.; Chang, E. K.; Louie S. G. *Phys. Rev. B* **1998**, *57*, 7027.
(32) Rappe, A.; Rabe, K.; Kaxiras, E.; Joannopoulos, J. D. *Phys. Rev. B* **1990**, *41*, 1227.
(33) Ireta, J.; Galván M. *J. Chem. Phys.* **1996**, *105*, 8231.
(34) Aldebert, P.; Traverse, J.-P. *J. Am. Ceram. Soc.* **1985**, *68*, 34.

(35) Teufer, G. *Acta Crystallogr.* **1962**, *115*, 1187.
(36) Gray, D. E. Ed. *American Institute of Physics Handbook*; McGraw-Hill: New York, 1972.
(37) Jansen, H. J. F. *Phys. Rev. B* **1991**, *43*, 7267.
(38) Kleinman, L.; Bylander, D. M. *Phys. Rev. Lett.* **1982**, *4*, 1425.
(39) Evarestov, R. A.; Smirnov, V. P. *Phys. Stat. Sol. (b)* **1983**, *119*, 9.
(40) Arias, T, A.; Payne, M. C.; and Joannopoulos, J. D. *Phys. Rev. B* **1992**, *45*, 1538.
(41) Cohen, M. L.; Schlüter, M.; Chelikowsky, J. R.; Louie, S. G. *Phys. Rev. B* **1975**, *12*, 5575.
(42) Kustov, L. M.; Kazansky, V. B.; Figueras, F.; Tichit, D. *J. Catal.* **1994**, *150*, 143.
(43) Boronat, M.; Viruela, P.; Corma, A. *J. Phys. Chem. B* **1997**, *101*, 10069.
(44) Hong, Z.; Fogash, K. B.; Watwe, R. M.; Kim, B.; Masqueda-Jiménez, B. I.; Natal-Santiago, M. A.; Hill, J. M.; Dumesic, J. A. *J. Catal.* **1998**, *178*, 489.
(45) Fukui, K. *Science* **1982**, *218*, 747.
(46) Hoffmann, R. *Rev. Mod. Phys.* **1988**, *60*, 601.
(47) Some authors have stress out the importance of hydride transfer in the transformation of hydrocarbons on SZ, see: Vera, C. R.; Pieck C. L.; Shimizu, K.; Querini, C. A.; Parera, J. M. *J. Catal.* **1999**, *187*, 39.
(48) Kazansky, V. B.; Senchinya, I. N. *J. Catal.* **1989**, *119*, 108.
(49) Hossain, Md. M.; Lin, Y. S.; Sugiyama, H.; Matsumoto, K. *J. Am. Chem. Soc.* **2000**, *122*, 172.
(50) Orlando, R.; Pisani, C.; Ruiz, E.; Sautet, *P. Surf. Sci.* **1992**, *275*, 482.
(51) Lindan, P. J. D.; Harrison, N. M.; Gillan, M. J. *Phys. Rev. Lett.* **1998**, *80*, 762.
(52) Gu, Y. M.; Bylander, D. M.; Kleinman, L. *Phys. Rev. B.* **1994**, *50*, 2227.
(53) Stowasser, R.; Hoffmann, R. *J. Am. Chem. Soc.* **1999**, *121*, 3414.
(54) Garza, J.; Nichols, J. A.; Dixon, D. A. *J. Chem. Phys.* **2000**, *112*, 7880.